The Effect of Diffusible Hydrogen in Weld Seams on the Mechanical and Corrosion Behaviour of S235JR Steel Parts in 3.5% NaCl

CATALINA SORINA PARFENE[1], GHEORGHE SOLOMON[1], DANIELA IONITA[2]*, IONELIA VOICULESCU[1], CLAUDIU BABIS[1], ION MIHAI VASILE[1]

[1] Politehnica University of Bucharest, Department of Materials Technology and Welding, 313 Splaiul Independentei Str., 060042, Bucharest, Romania

[2] Politehnica University of Bucharest, Department of General Chemistry,1-3 Gh.Polizu Str., 011061, Bucharest, Romania

It is known the bad influence on the behaviour of diffusible hydrogen in case of the cold cracking of steels. A very important issue for the welded structures is to ensure resilience and breaking energy at a certain value, even at negative temperatures, the paper aims is to highlight the influence of diffusible hydrogen on the mechanical and toughness characteristics. Another aim of this paper was the study of the influence of diffusible hydrogen on corrosion behaviour in the case of both welded and non-welded S235JR steel samples manufactured.

Keywords: diffusible hydrogen, electrolytic hydrogen charging, resilience, breaking energy, welded seams, corrosion

Numerous experimental studies focused on hydrogen deformation interactions in low alloy steels [1-3], clearly show significant effects of hydrogen on the plasticity of these alloys [4, 5].

Establishing the corrosion resistance for metallic alloys is very important to determine its viability for a particular application. The low alloyed steels are probably the most widely known and commonly used materials of construction for corrosion resistance [6]. For many years this was the only material available to provide any degree of resistance to corrosive attack. During corrosion processes part of the reduced hydrogen can be absorbed on the metal surface and diffuse into low alloy steel [7 - 9] while the rest of hydrogen forms gas molecules and broadcast. Hydrogen dissolved in metals significantly affects their mechanical properties, composition and structure of passive films. For instance, hydrogen can cause low yield and fracture stresses in steels [10]. Studies showed that hydrogen affects steel corrosion rates [11], as in pitting corrosion [12].

Diffusible hydrogen is responsible for the cold cracks in the welded joints[13, 14]. It is well known that the existence of hydrogen has detrimental effects on the mechanical properties of S 235 JR steel, such as reducing both ductility and fracture resistance, causing hydrogen embrittlement, blisters, and hydrogen-induced cracking [15,16]. In a corrosive environment, hydrogen can facilitate crack initiation and propagation by forming an active dissolution path and enhancing the local dissolution at the crack-tip [16].

Hence, the present research aims at analyzing the impact of diffusible hydrogen on the mechanical characteristics [17 - 19], tenacity and plasticity for both the hydrogen undergoing welding and the hydrogen charge of samples by means of electrolysis in case of specimens made of a general purpose steel S 235 JR symbols according to EN 10025-2:2004 [20, 21].

Formation of hydrogen

Hydrogen is most frequently formed during pickling in mineral acids, cathodic electrolytic degreasing, electroplating processes, also during oxidation (corrosion) of the material, welding and phosphating [22].

In most cases it involves catodic reduction. For example, during pickling in mineral acids (NH_3, H_2SO_4, HCl) the relevant anodic step, the dissolution of metal, takes place as the formation of hydrogen [22].

In contrast, during electrolytic degreasing and galvanizing the formation of hydrogen – and dissolution of metal, if any- takes place separately at the anode (1) and (2):

in acidic medium: $2H_3O^+ + 2e^- \rightarrow H_2 \uparrow + 2H_2O$ (1)

in alcalin medium: $2H_2O^+ + 2e^- \rightarrow H_2 \uparrow + 2OH$ (2)

Subsequent reaction take place step by step. Hydroxyl ions to separate one by one, water molecules are broken down one after the other. In any case, atomic hydrogen is formed first (3), [22]:

$$H_3O^+ + e^- \rightarrow H + H_2O \quad (3)$$

Atomic hydrogen necessarily needs to form a bond and is therefore reactive. When it meets another hydrogen atom, they form a bond.

In this case we speak about absorbed (atomic) hydrogen H_ad. Adsorbed atomic hydrogen can bind with another of its kind to form a molecule of H_2, which is eventually released in the form of gas bubbles and no longer poses any threat to the base material. However, absorbed atomic hydrogen can also diffuse into the material and damage its structure (4), [22].

Formation of gaseous H_2:

$$2H_{ad} \rightarrow H_2 \uparrow \; or \; H_{ad} + H_3O^+ + e^- \rightarrow H_2 \uparrow + H_2O \quad (4)$$

Diffusion into the material :$H\_ad \rightarrow H\_mat$

* *email: md_ionita@yahoo.com*

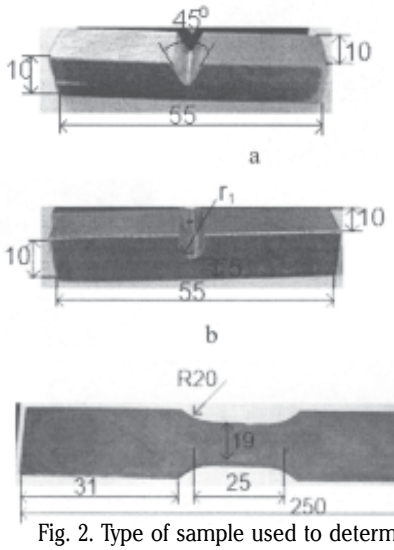

Fig.1. Types of samples used to determine the plasticity/tenacity characteristics

Fig. 2. Type of sample used to determine the mechanical characteristics

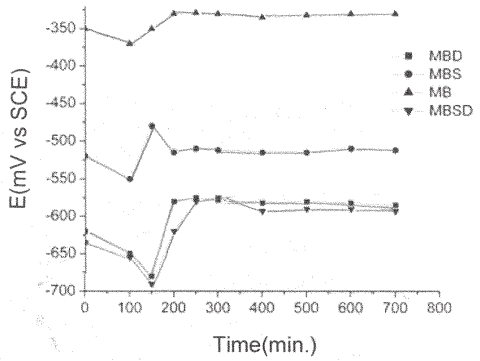

Fig.3. Open circuit potential variation with time for al Samples in 3.5% NaCl solution

Experimental part

The dimensions of V-shaped and U-shaped samples, to determine the tenacity and plasticity characteristics, are 10 x 10 x 55 mm, their shape is illustrated in figures 1a and 1 b.

The dimensions of samples required for the determination of mechanical characteristics in the case of static tension and fracture point are 10 x 31 x 250 mm, their shape is illustrated in figure 2.

Table 1 shows the chemical composition of S235JR type of steel and table 2 reveals the mechanical characteristics.

Two sets of samples were used to analyze the effect of diffusible hydrogen on the plasticity and tenacity properties, similar to those illustrated in figure 1, consisting of 8 pieces each. One set includes V-shaped samples and KV [J] as breaking energy and the other set is made of U-shaped samples and the following: resilience values KCU [J/cm^2] at environmental temperature of 25°C, Cr [%] crystallinity, Fb [%] fiber texture and cross compressions T [%]. The samples were marked as P1V…P8V for the V-shaped set and P1U…P8U for the U-shaped set, respectively, in conformity with the specifications shown in table 3.

A key observation is that, in the case of electrolytic hydrogen charging, the charging took 10 h for samples P2 and P6, 20 h for samples P3 and P7 and 30 h for samples P4 and P8. The effect of diffusible hydrogen was evident in the case of both the samples made of unwelded base material (P1V/U; P2V/U; P3V/U; P4V/U) as well as of the welded base material ones (P5V/U; P6V/U; P7V/U; P8V/U), on the tenacity characteristics – V-shaped samples and plasticity – U-shaped samples. It is noteworthy that, an increase in the charging period led to a higher amount of diffusible hydrogen. Hence, the results obtained for tenacity and plasticity were compared for all types of samples designed according to the specifications illustrated in table 3.

One of them was marked T1 and made of base material, other three marked as T2; T3 and T4 made of hydrogen base material and one T5, made of welded base material and the last marked as T6; T7 and T8 were made of welded electrolytically charged base material.

Weld charge was achieved by means of a coated electrode type cellulosic E6010 with a base coating in conformity with AWS A5.1-04.

This particular type of electrode was needed in order to introduce large quantities of hydrogen during welding. The chemical composition of the deposited metal is shown in table 4 and the mechanical properties are revealed in table 5.

Material name	C [%]	Mn [%]	S [%]	P [%]	Cu [%]	Other [%]
Steel for boilers and pressure vessels	max. 0.17	1.40	max. 0.045	max. 0.045	Max. 0,45	N = 0.012

Table 1
CHEMICAL COMPOSITION OF S235JR, ACCORDING TO SR EN 10025-2:2004

Material	$R_{p\,0.2}$ [N/mm^2]	R_m [N/mm^2]	A_5 [%]	Hardness HB	KV [J]
S235JR	235	360-510	Min. 20	104-154	27

Table 2
MECHANICAL CHARACTERISTICS OF S235JR TYPE OF STEEL

Type of sample	P1V P1U	P2V P2U	P3V P3U	P4V P4U	P5V P5U	P6V P6U	P7V P7U	P8V P8U
Sample characteristics	Base Material MB	Base material electrolytically charged with hydrogen diffusible MBD			Welded base material MBS	Welded and electrolytically hydrogen charged MBSD material		

Table 3
TYPES OF SAMPLES USED TO DETERMINE THE TENACITY AND PLASTICITY FEATURES

Electrode code	Chemical elements		
AWS A5.1-04 E6010	C max.[%] 0.12	Si[%] 0.14	Mn[%] 0.5

Table 4
THE CHEMICAL COMPOSITION OF THE DEPOSITED METAL BY MEANS OF THE ELECTRODE E 6010

Electrode code	Mechanical characteristics		
AWS A5.1-04 E6010	Yield strenght [MPa] 410	Tension resistence [MPa] 495	Elongation [%] 26

Table 5
MECHANICAL CHARACTERISTIC OF ELECTRODE E 6010

Evaluation by electrochemical methods

The experimental setup for the electrochemical measurement consisted of a three electrode glass, a standard Ag/AgCl was used as the reference electrode, and the counter electrode consisted of two graphite rods positioned symmetrically relative to the working electrode (test specimen), supplying the current. The exposed surface area of the working electrode was 1.0 cm^2. Electrochemical measurements were carried out in NaCl 3.5% solution, the most common electrolyte used for corrosion testing and evaluation , at 25 ± 1^0C employing a potentiostat/galvanostat – Voltalab 40. The open circuit potential (OCP) values of the test specimen were monitored for immersion upto 72 h.

The polarization curves were recorded at a potential scan from –0.2 V to + 0.3V versus open circuit potential and a scan rate of 2 mV/s. Quantitative analyses from the polarization curves were made to determine Ecorr (corrosion potential), Icorr (corrosion current density), and cathodic and anodic Tafel slopes. The corrosion rate, CR (rate of metal dissolution), expressed in millimeters per year was determined with a standard equation [23].

Corrosion tests were performed on base material, welded base material and base material electrolytically charged with hydrogen diffusible for 10, 20 and 30 h.

Results and discussions

In the aftermath of various tests and experiments on fractures by means of a 15 kg mass Charpy impact testing machine, the following KV breaking energy values were achieved for V-shaped samples as shown in table 6.

Table 7 indicates the values of the breaking energy obtained,W_0 under shock bending by means of the 15 kg mass Charpy impact testing machine, at 25°C, as well as resilience values KCU, calculated based on relation 5:

$$KCU = \frac{W_0}{S_0} \quad (5)$$

where KCU- is the resilience;W_o- represents the breaking energy and S_o- is the initial cutting of the sample.

The values of the geometrical elements of the brittle breaking sections a_f and b_f, determined for each U-shaped sample, after breaking, by means of a 1/10 beam compass, are shown in table 8. The same table indicates the values of section brittle baking areas S_f, ductile S_d respectively, according to relations 6 and 7.

$$S_f = a_f x b_f \quad (6)$$

$$S_d = S_0 - S_f \quad (7)$$

Once the section areas for brittle and ductile breaking determined, crystallinity C_r, fiber texture F_b and cross compression T were calculated, based on relations 8; 9 and 10, for U-shaped samples. The corresponding values are indicated in table 9. For the T cross compression, b and b1 values were used, determined by means of a 1/10 beam compass (table 8).

$$C_r = \frac{S_f}{S_0} x100 \quad (8)$$

$$F_b = \frac{S_d}{S_0} x100 \quad (9)$$

$$T = \frac{b - b_1}{b} x100 \quad (10)$$

The results of the research on tensile test are illustrated in table 10.

Electrochemical results

One simple way to study the corrosion behaviour, i.e.film formation and passivation of alloys in a solution, is to monitor the open-circuit electrode potential (OCP) as a function of time. The shift of potential in the positive direction indicates the formation of a passive film, and a steady state potential indicates that the surface remains intact and protective. A drop of potential in the negative direction indicates breaks in the film, dissolution of the film, or no film formation [24].

Figure 3 shows the OCP curves versus time obtained for steel in aerated stagnant 3.5 wt% NaCl solutions.

It is seen from figure 3 that the potential for all studied materials tend towards more negative values from the first moment of electrode immersion as a result of the dissolution of an air oxide film that was formed on the electrode before its immersion in the solution. The potential then abruptly shifted from -680 mV to -560 mV for base material electrolytically charged with hydrogen, from -550 mV to -510 mV for welded base material and from -370

Sampling	MB		MBD		MBS		MBSD	
Sample	P1V	P2V	P3V	P4V	P5V	P6V	P7V	P8V
Charge duration [h]	0	10	20	30	0	10	20	30
KV [J]	75	71	67	64	45	41	38	34

Table 6
VALUES OF BREAKING ENERGY KV FOR V-SHAPED SAMPLES

Sampling	MB		MBD		MBS		MBSD	
Sample	P1U	P2 U	P3U	P4 U	P5U	P6U	P7U	P8U
Charge duration [h]	0	10	20	30	0	10	20	30
S_0 [mm^2]	50	50	50	50	50	50	50	50
W_0 [J]	95	90	85	81	57	52	47	42
KCU [J/cm^2]	190	180	170	162	114	104	94	84

Table 7
RESILIENCE VALUES KCU OBTAINED FOR U-SHAPED SAMPLES

Sampling	MB		MBD		MBS		MBSD	
Sample	P1U	P2U	P3U	P4U	P5U	P6U	P7U	P8U
Sample charge duration [h]	0	10	20	30	0	10	20	30
a_f [mm]	5.8	6	6	5.9	6.5	6.42	6.08	6
b_f [mm]	1.6	1.6	1.7	1.8	2.0	2.1	2.3	2.4
S_f [mm^2]	9.3	9.8	10.2	10.7	13	13.5	14	14.4
S_d [mm^2]	40.7	40.2	39.8	39.3	37	36.5	36	35.6

Table 8
VALUES OF THE GEOMETRICAL ELEMENTS FOR BREAKING SECTIONS OF THE U-SHAPED SAMPLES

Sampling	MB		MBD		MBS		MBSD	
Sample	P1U	P2U	P3U	P4U	P5U	P6U	P7U	P8U
Charge duration [h]	0	10	20	30	0	10	20	30
b [mm]	10	10	10	10	10	10	10	10
b_1 [mm]	8.7	8.9	9.1	9.2	9.4	9.7	9.8	9.8
C_r [%]	18.6	19.6	20.4	21.4	26	27	28	28.8
F_b [%]	81.4	80.4	79.6	78.6	74	73	72	71.2
T [%]	13	11	9	8	5	3	2	2

Table 9
CRYSTALLINITY VALUES C_r, FIBER TEXTURE F_b AND CROSS COMPRESSION T FOR U-SHAPED mSAMPLES

Sampling	MB		MBD		MBS		MBSD	
Sample	T1	T2	T3	T4	T5	T6	T7	T8U
Charge duration [h]	0	10	20	30	0	10	20	30
Rm [N/mm^2]	360	355	350	355	355	345	340	345

Table 10
VALUES OFBREAKING TENSION Rm

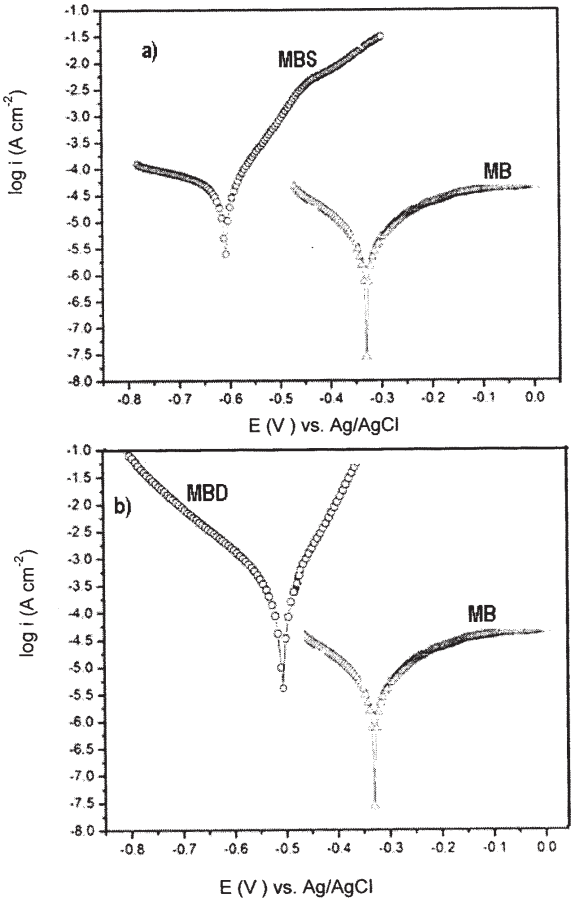

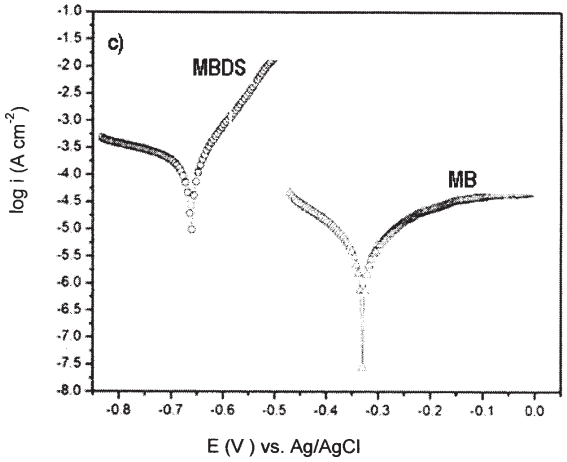

Fig. 4. Tafel curves for a) MB and MBS; b) MB and MBD; c) MB and MBDS in 3.5% NaCl solution

mV to -325 mV for base material. This positive potential shift indicates the passivation of the steel surface due to the formation of an oxide film. Further increasing the time of the experiment led to a rapid negative potential shift, which might have resulted from the dissolution of the formed oxide film under the influence of the aggressive chloride ions attack. The most electronegative potentials were recorded for welded and electrolytically hydrogen charged material (-690mV). After about 250 min the potential reaches a steady state for all studied materials, indicating that the steel surface was under equilibrium between dissolution and protection via the formation of an oxide film and/or a layer of corrosion products.

In figures 4 are presented the polarization curves for all materials (MB, MBS, MBD, MBSD) after testing in 3.5% NaCl solution.

Each of the potentiodynamic polarization curves in the range of potentials tested consists of two parts: the cathodic and anodic segments. Part of the reduction process corresponds to the cathodic corrosive components of H^+ and O_2 occurring on the metal surface. Test results after the corrosion test of non-alloyed steel S235JR in 3.5% NaCl are presented in table 11.

It is notice that the corrosion potential shifts towards more cathodic potential in the following order: $E_{MDBS} > E_{MBS} > E_{MBD} > E_{MB}$. This results are in concordance with OCP measurement.

An alloy that prone to passivity will have the value of ba higher than bc, while an alloy that corrodes will have ba lower then bc [25]. For welded and electrolytically hydrogen charged material was recoded the highest value of bc,

Materials	β_a [V/dec]	β_c [V/dec]	E_{corr} [mV]	I_{corr} [A/cm^2]	CR [mm/year]
MB	0.178	0.158	-329	$4.621 \cdot 10^{-6}$	0.05
MBS	0.084	0.258	-608	$4.425 \cdot 10^{-5}$	0.51
MBD	0.081	0.346	-515	$6.227 \cdot 10^{-4}$	7.31
MBSD	0.102	0.432	-656	$9.138 \cdot 10^{-4}$	10.72

Table 11
MAIN PARAMETERS OF CORROSION PROCESS FROM STEEL S235JR

corresponding with the highest value of corrosion rate. In concordance with the classification of corrosion behaviour of metallic materials according to stability and corrosion resistance [26, 27] the base material is "stable", weld base material is "relative stable", material electrolytically charged with hydrogen and welded and electrolytically hydrogen charged material are "low stability" materials.

Conclusions

The following conclusions can be drawn with regard to the data indicated in the tables:

- a decrease in the KV and KCU plasticity values, when a simple MB base material is changed for an MBD electrolytically hydrogen charged material, for an MBS welded base material and then for welded and electrolytically hydrogen charged MBSD material, provided the charging duration prolongs from 10 to 30 h. The lowest values are achieved for welded base materials as compared to the values of the MB base material

- these values do not differ significantly for the same hydrogen charge duration. Hence, resilience tests do not prove the hydrogen embrittlement of a sample;

- a decrease in fiber texture Fb and an increase in crystallinity with the change of MB to MBD; MBS with the prolonging of charge duration from 10 to 20 and even 30 hours; a key observation is the drop in cross compression provided the prolonging of hydrogen charge duration;

- a drop in tenacity and plasticity characteristics with the prolonging of hydrogen charge duration is due to a big amount of hydrogen (positive ions) introduced into the base material or the welded structure. The internal pressure grows and embrittlement of the area occurs. As the research reveals, this can be proved in the case of dynamic stress under shock bending;

- the lowest values of the KV breaking energy, KCU resilience and T cross compression are obtained for welded and hydrogen charged materials, since, by welding, a high amount of hydrogen is introduced from the coated electrode (manual electric arc welding), to which electrolytic hydrogen charge is added. Likewise, internal weld tensions must be considered, since, combined with diffusible hydrogen, can render disastrous consequences;

- regarding the tests on static tension, the results have revealed that breaking tension does not vary significantly with the prolonging of diffusible hydrogen charge duration, a possible explanation is the relatively high rate of deformation which does not allow embrittlement of the samples in the short run, during charging.

- the incorporation of hydrogen into S 235 JR steel leads to formation of highly defective passive films that have poor resistance to corrosion.

-hydrogen charged sample corrode at lower potential; this indicates, that as results there follows a degradation of thin passive film on the S235JR steel.

References

1HERTZBERG, RICHARD W. Deformation and Fracture Mechanics of Engineering Materials. NewYork: John Wiley & Sons, Inc., 1996;

2 KIM, C.D. Metals Handbook, Vol. 11, Failure Analysis, 9th Edition. Metals Park, OH: ASM International, 1986, p. 245

2RAYMOND, L., Hydrogen Embrittlement: Prevention and Control. Philadelphia, PA. ASTM, 1988

4 GAVRILJUK, V.G., SHIVANYUK, V.N., FOCT, J., Acta Mater., 51 (5), 2003, p.1293

5 SHIVANYUK, V.N., FOCT, J., GAVRILJUK, V.G., Mater. Sci. Eng., A 300 (1–2), 2001, p.284

6 XIANGBO, L., JIA, W., WEI, W., HONGREN, W., Mat. and Corr., 58, 2007, p.29

7. QIAO, L.J., CHU, W.Y., HSIAO, C.M., Scr. Metall., 22, 1988, p.627

8 KIM, Y.P., FREGONESE, M., MAZILLE, H., FERON, D., SANTARINI, G., Corros. Sci., 48, 2006, p. 3945

9 LU, B.T., Fatigue & Fracture of Engineering Materials & Structures, 36, 2013, p. 660

10 MARSH, P.G., GERBERICH, W.W., R.H. Jones (Ed.), Stress Corrosion Cracking, ASM International, Ohio, 1992, pp. 63.

11 QIAO, L.J., LUO, J.L., Corr., 54, 1998, p.281

12 FREGONESE, M., IDRISSI, H., MAZILLE, H., RENAUD, L., CETRE, Y., Corr. Sci., 43, 2001, p.627

13 MICLOSI, V. , Heat treatment related fusion welding of steels, vol. I, Ed. Sudura, 2003, Timisoara, p. 69

14 VOICULESCU, I., Hydrogen in steel welded construction, ISBN 973-718-181-6, Ed.Printech, 2005, Bucharest, p.5

15 SZUMMER, A., JEZIERSKA, E., LUBLINSKA, J., Alloys Comp., 356, 1999, p.293

16 LUO, H., DONG, C. F., LIU, Z. Y., MAHA, M. T. J., LI, X. G., Mat. and Corr., 64**,** 2013, p.26

17. KNOTT, J.F., Fundamentals of fractures mechanics, Butterworth's, London, Ch 8, 1973 p.331

18. HIRTH, J.P., Effect of hydrogen on the properties of iron and steel, Metal.Trans.A, 11, 1980, p.861

19. HIRTH, J.P, ONYEWUENYI, O.A., LOUTHAN, M.R., MCNITT. R.P., SISSON, R.D., In environmental degradation of engineering materials in hydrogen, Eds. VPI Press, Blacksburg, p.133

20 N.OHTSUKA, Y. SHIND, A.MAKITA, ICEM 14 - 14th International Conference on Experimental Mechanics, Poitiers, France, Edited by FabriceBrémand; EPJ Web of Conferences, Volume 6, id.14004

21 PILLOT, S., BOURGES, P., MASSO, G.,COUDREUSE, L., Toussait, Corr., 2008

22 VOJKOVSKY, K., KUDLACEK, J., FALTYNKOVA, A., International Conference on Innovative Technologies, IN-TECH, ISBN 978-953-6326-88-4, Budapest, 2013, p.373

23 KETCHAM, J., FRANCE, W. D., WILEY J., New York, 1971, p. 173

24 I.GURAPPA, Mat. Charac., 49, 2002, p.73

25 MANSFELD,F., ElectrochemSoc, 120, 1973, p.515.

26 VASILESCU, M., VASILESCU, I., REV. CHIM. (Bucharest), **60,** no. 1., 2009,
p. 23

27 UHLIGH, HH., Corr. and Corr. Cont., New York, 1985, p. 252

Manuscript reeived: 16.12.2013